AGU ADVANCING EARTH AND SPACE SCIENCE

Geophysical Research Letters

RESEARCH LETTER
10.1029/2020GL087351

Investigating the Nutrient Landscape in a Coastal Upwelling Region and Its Relationship to the Biological Carbon Pump

M.R. Stukel[1,2] and K.A. Barbeau[3]

[1]Department of Earth, Ocean, and Atmospheric Science, Florida State University, Tallahassee, FL, USA, [2]Center for Ocean-Atmospheric Prediction Studies, Florida State University, Tallahassee, FL, USA, [3]Scripps Institution of Oceanography, University of California San Diego, San Diego, CA, USA

Key Points:
- Dominant modes of nutrient variability included an onshore-offshore trophic gradient and Fe-stressed versus Fe-replete conditions
- Sinking particle flux was correlated with high surface nutrient concentrations, Fe stress, and low PO_4^{3-}:NO_3^- and $Si(OH)_4$:NO_3^- water
- Nutrient landscape was more predictive of vertical carbon export than net primary production was

Supporting Information:
- Supporting Information S1
- Table S1

Correspondence to:
M. R. Stukel,
mstukel@fsu.edu

Citation:
Stukel, M. R., & Barbeau, K. A. (2020). Investigating the nutrient landscape in a coastal upwelling region and its relationship to the biological carbon pump. *Geophysical Research Letters*, *47*, e2020GL087351. https://doi.org/10.1029/2020GL087351

Received 1 FEB 2020
Accepted 25 FEB 2020
Accepted article online 29 FEB 2020

Abstract We investigated nutrient patterns and their relationship to vertical carbon export using results from 38 Lagrangian experiments in the California Current Ecosystem. The dominant mode of variability reflected onshore-offshore nutrient gradients. A secondary mode of variability was correlated with silica excess and dissolved iron and likely reflects regional patterns of iron limitation. The biological carbon pump was enhanced in high-nutrient and Fe-stressed regions. Patterns in the nutrient landscape proved to be better predictors of the vertical flux of sinking particles than contemporaneous measurements of net primary production. Our results suggest an important role for Fe-stressed diatoms in vertical carbon flux. They also suggest that either preferential recycling of N or non-Redfieldian nutrient uptake by diatoms may lead to high PO_4^{3-}:NO_3^- and $Si(OH)_4$:NO_3^- ratios, following export of P- and Si-enriched organic matter. Increased export following Fe stress may partially explain inverse relationships between net primary productivity and export efficiency.

Plain Language Summary The productivity of marine ecosystems is limited by the availability of macronutrients (nitrogen and phosphorus) and trace elements (iron) in the sunlit surface ocean. The ocean's ability to absorb atmospheric carbon dioxide through the "biological carbon pump" is further constrained by the rates at which oceanic upwelling naturally fertilizes the surface ocean with "new" nitrogen contained in nutrient-rich deep water. We investigated patterns in nutrient distributions during 38 experiments in the California Current Ecosystem. In these experiments, we followed biological communities as they were transported with the currents and measured nutrients, primary productivity, and the export of organic carbon contained in sinking particles. Our results indicate that nutrient concentrations may be a useful predictor of rates of carbon export and that iron stress increased the efficiency with which organic carbon created by algae is transported to the deep ocean. This increased carbon export efficiency likely results from physiological changes within diatoms that lead to thicker silica shells relative to organic carbon content.

1. Introduction

Macronutrient and micronutrient distributions limit marine productivity and shape plankton community dynamics (Dugdale, 1967; Moore et al., 2013). The macronutrients NO_3^-, NH_4^+, and PO_4^{3-} are necessary and often limiting for all phytoplankton taxa, while silicic acid is required by diatoms, which are often the dominant taxa in coastal regions (Benitez-Nelson, 2000; Davey et al., 2008; Dugdale & Goering, 1967). Although all phytoplankton taxa require Fe and other trace metals, these trace elements are typically most important for the growth of large phytoplankton (e.g., diatoms) in open-ocean regions with limited dust deposition (Behrenfeld et al., 1996; de Baar et al., 2005; Falkowski et al., 1998). The supply of "new" nutrients (i.e., nutrients that are not produced through internal ecosystem recycling) to the euphotic zone is also a fundamental constraint on the biological carbon pump (BCP). The BCP is a suite of processes that convert carbon dioxide into organic carbon and then sequester this organic carbon in the deep ocean for periods of decades to millennia (Boyd et al., 2019; Eppley & Peterson, 1979; Volk & Hoffert, 1985). The BCP is fundamentally linked to nitrogen (in addition to phosphorus and Fe) supply to the euphotic zone as a result of the relatively constant elemental stoichiometry of marine organic matter (Redfield, 1934; Takahashi et al., 1985). However, the BCP is driven by ecological interactions that combine organic matter into sinking particles and aggregates, create recalcitrant organic matter that is eventually subducted, or actively transport

carbon to depth during vertical migrations (Buesseler & Boyd, 2009; Ducklow et al., 2001; Steinberg & Landry, 2017). Quantifying the interactions between nutrient supply, availability, stoichiometry, and the BCP is an important part of understanding future changes in marine carbon sequestration as a result of climate change (Boyd, 2015; Omta et al., 2006; Passow & Carlson, 2012).

Understanding nutrient dynamics and the BCP in coastal ecosystems is particularly important, because of the high biomass, productivity, and CO_2 fluxes in these regions (Ducklow & McCallister, 2004). Eastern boundary current upwelling ecosystems are some of the most productive ecosystems on our planet and are expected to respond to increasing land-sea temperature gradients (Bakun, 1990; Sydeman et al., 2014). The southern California Current Ecosystem (CCE) is a coastal upwelling biome that supports a high biomass of plankton and higher trophic levels (Ohman et al., 2013). It is a region that experiences substantial interannual and decadal variability (Chelton et al., 1982; Lavaniegos & Ohman, 2007; McGowan et al., 2003). It is expected to receive enhanced nutrient supply as a result of climate change, although the impact of upwelling on nutrient supply is complicated by documented changes in the source water for upwelling (Bograd et al., 2015; Rykaczewski & Dunne, 2010).

Despite being a coastal biome, the narrow shelf of the CCE leads to relatively weak fluxes of Fe into the euphotic zone (Bruland et al., 2001; King & Barbeau, 2011). As a result, large regions of the CCE are believed to experience Fe limitation or Fe and N colimitation (Hutchins & Bruland, 1998; King & Barbeau, 2007). Fe limitation in the CCE has been diagnosed through observations of Si_{ex}, where $Si_{ex} = [Si(OH)_4] - [NO_3^-] \times R_{Si:NO3}$, and $R_{Si:NO3}$ is the ratio of $Si:NO_3^-$ in upwelled waters (Hogle et al., 2018). Negative Si_{ex} is believed to be created when Fe-starved diatoms take up excess Si relative to NO_3^- (Franck et al., 2000; Hutchins & Bruland, 1998). The mineral ballasting provided by these dense diatoms is believed to lead to increased export flux in the CCE (Brzezinski et al., 2015; Stukel et al., 2017), although the export flux is mediated by mesozooplankton that repackages diatoms into rapidly sinking fecal pellets (Morrow et al., 2018; Stukel et al., 2013). Similarly, export flux is enhanced in the deep Atlantic, following Fe introduction by Saharan dust (Pabortsava et al., 2017). Si_{ex} has been used to show that Fe limitation may be a pervasive feature of subsurface chlorophyll maxima in the CCE (Hogle et al., 2018). However, Si_{ex} can also be created without Fe limitation if N is preferentially remineralized (relative to Si) from sinking particles and diatoms utilize recycled NH_4^+.

To investigate nutrient patterns and their impact on carbon export, we utilize results from 38 two- to five-day Lagrangian experiments conducted on eight different cruises of the CCE Long-Term Ecological Research (LTER) program. These Lagrangian experiments allowed us to simultaneously determine nutrient concentration profiles, measure net primary production (NPP), and deploy sediment traps to quantify sinking carbon flux. We use principal component analysis (PCA) to determine that the primary driver of nutrient variability is coastal upwelling, while the secondary mode is Fe limitation. We further show that the nutrient landscape is a better predictor of carbon export than NPP.

2. Materials and Methods

2.1. In Situ Sampling

In situ measurements were made during quasi-Lagrangian experiments (hereafter "cycles") of the CCE LTER program (King et al., 2012; Landry et al., 2009). During these cycles, water parcels (ranging from coastal eutrophic to oligotrophic offshore communities) were marked with an array consisting of a surface, satellite-enabled float, and a 3 × 1-m drogue. Two types of arrays were deployed. One consisted of a set of attachment points for mesh bags containing incubation bottles (Landry et al., 2009). Incubations (for $H^{14}CO_3$ uptake NPP, among other measurements) were conducted at six to eight depths spanning the euphotic zone (Morrow et al., 2018). The second array supported drifting sediment traps deployed at one to three depths beneath the euphotic zone (Stukel et al., 2013). For additional methodological details, see supporting information.

Lagrangian sampling was conducted on eight cruises of the CCE LTER program, although sampling plans varied as a result of differing cruise objectives. On the P0605 (May 2006), P0704 (April 2007), and P0810 (October 2008) cruises, our goal was to investigate variability in plankton dynamics in the region. Hence we sampled homogeneous (i.e., nonfrontal) water parcels spanning coastal to offshore conditions (Landry

et al., 2012; Stukel et al., 2012). On the P1408 (August 2014) and P1604 (April 2016) cruises, our goal was to investigate system responses to anomalous warming associated with the 2014–2015 North Pacific warm anomaly and ensuing El Niño using similar sampling patterns (Kelly et al., 2018; Morrow et al., 2018; Nickels & Ohman, 2018). On the P1106 (June 2011) and P1208 (August 2012) cruises, we sought to determine ecosystem responses to mesoscale fronts and hence conducted cycles within and to either side of strong frontal gradients (de Verneil & Franks, 2015; Krause et al., 2015; Stukel et al., 2017). On the P1706 (June 2017) cruise, we investigated cross-shore transport mediated by a coastal filament, and hence cycles from this cruise represent a progression from coastal upwelling conditions to bloom decay as water is advected offshore.

Samples for macronutrients were taken from two CTD-Niskin rosette casts per day on each cycle. Samples were filtered through a 0.1-μm filter and stored at −20°C until analysis on land. $NO_3^- + NO_2^-$ (hereafter NO_3^-), PO_4^{3-}, $Si(OH)_4$, and NH_3^+ were determined colorimetrically using an autoanalyzer (Parsons et al., 1984). Dissolved Fe (dFe) was measured on samples collected using either trace metal clean Go-Flo bottles or a trace metal clean rosette (Bundy et al., 2016; King et al., 2012). dFe was measured using a chemiluminescent flow injection approach (King & Barbeau, 2011). SAFe standards (Johnson et al., 2007) were analyzed as an independent validation of the method.

Vertical carbon flux was measured using VERTEX-style sediment traps (Knauer et al., 1979) and ^{238}U–^{234}Th disequilibrium (Waples et al., 2006). Sediment traps (8:1 aspect ratio with a baffle on top consisting of 14 smaller, beveled tubes with similar aspect ratio) were consistently deployed at a depth of 100 m. Additional traps were deployed near the base of the euphotic zone (when the euphotic zone was shallower than 80 m) and at 150 m (on cruises from 2014 onward). Traps were deployed with a saltwater brine (filtered seawater + 50-g L^{-1} NaCl) poisoned with (0.4%) formaldehyde. After recovery, >200-μm swimming mesozooplankton were removed from the samples, and samples were filtered for carbon analyses by Carbon Hydrogen Nitrogen (CHN) analyzer and biogenic Si analyses using a NaOH digestion approach (Krause et al., 2015; Stukel et al., 2019). ^{234}Th was measured using standard small volume approaches (Benitez-Nelson et al., 2001; Pike et al., 2005). ^{238}U was estimated from salinity (Owens et al., 2011), and ^{234}Th export was determined from ^{238}U–^{234}Th deficiency using a steady-state one-dimensional approximation (Savoye et al., 2006). Excellent agreement was found between ^{234}Th flux into sediment traps and ^{238}U–^{234}Th disequilibrium, suggesting no substantial under- or over-collection bias by sediment traps (Stukel & Kelly, 2019; Stukel et al., 2019). Because sediment trap integration time more closely matches that of other measurements, we use sediment trap results for all cruises except P0605 (when sediment traps were not available). For additional details, see Stukel et al. (2019) and Morrow et al. (2018).

2.2. Statistical Analyses

To investigate the nutrient landscape in the CCE, we used 11 nutrient indices: surface $[NO_3^-]$, $[NH_4^+]$, $[PO_4^{3-}]$, $[Si(OH)_3]$, [dFe], Si_{ex}, and N* (=$[NO_3^-] - 16 \times [PO_4^{3-}]$), and the depths of the nitracline, phosphocline, silicocline, and ferrocline. We used probabilistic PCA (Tipping & Bishop, 1999) to explore nutrient patterns after normalization of the data. To investigate the correlations between nutrient principal components (PCs) and vertical carbon flux, we used stepwise linear regression (Draper & Smith, 1998) with the PCs as independent variables and $\log_{10}$ transformed carbon flux as the dependent variable. To quantitatively compare the predictive ability of regressions based on nutrient dynamics to regressions based on NPP, we used nonparametric bootstrapping approaches. Briefly, 10^5 random data sets were created by sampling half of the 36 Lagrangian cycles that included carbon flux measurements (included data set). These data sets were used to quantify separate ordinary least squares (OLS) regressions using nutrient PCs or $\log_{10}$(NPP) as independent variables and $\log_{10}$(Export) as the dependent variable. OLS regression was used, as recommended by Sokal and Rohlf (2012), because only OLS minimizes the sum of squared residuals in the dependent variable, thus making it the most appropriate approach when used for prediction. We caution, however, that OLS is not appropriate if the goal is to investigate the functional relationship (i.e., slope) between the dependent and independent variables, and the independent variable is not controlled. Predicted values of carbon export were computed for the 18 Lagrangian cycles not included in determining the regression. The sum of squared model misfits was then computed for the nutrient-based regressions and the NPP-based regression. For additional details, see supporting information.

3. Results and Discussion

3.1. The Nutrient Landscape in the CCE

Nutrient conditions encountered across the 38 Lagrangian cycles were highly variable. Cycle average surface NO_3^- ranged from 0.01 to 7.8 μmol L^{-1}, with a standard deviation of 2.5 μmol L^{-1}. Surface NH_4^+ ranged from undetectable to 1.8 μmol L^{-1} but was typically in the range of 0.05 to 0.3 μmol L^{-1}. Surface PO_4^{3-} was likely not limiting for phytoplankton and ranged from 0.16 to 0.78 μmol L^{-1}, with consistently negative N* values. Surface $Si(OH)_4$ showed similar variability to NO_3^-, ranging from 0.22 to 11.2 μmol L^{-1} with a standard deviation of 2.6 μmol L^{-1} although it was not drawn down as low as NO_3^-. Si_{ex} was typically positive at the surface but was negative on seven cycles, reaching values as low as −5.0 μmol L^{-1}. Surface dFe ranged from 0.069 to 1.3 nmol L^{-1}. The cycle average depth of the nitracline varied from 17 to 152 m. Nitracline, phosphocline, silicocline, and ferrocline depths were highly correlated.

Probabilistic PCA reveals the dominant modes of variability in the nutrient landscape. The first PC had strong negative coefficients for all surface nutrient concentrations and strong positive coefficients for the depth of all nutriclines and explained 50% of the variability in the data (Figure 1a and supporting information Table S1). It split the samples along a trophic gradient in which negative scores for PC1 were indicative of nutrient-rich upwelled waters and positive scores reflected nutrient-depleted oligotrophic conditions. PC1 mostly reflected the strong cross-shore gradients in the CCE, with negative scores near the Point Conception upwelling center and positive scores offshore. However, there was intercruise variability in the ranges of upwelling and oligotrophic conditions (Figure 1b). Most noticeably, on the P1408 cruise all cycles had positive PC1, because upwelling was suppressed by region-wide warming (Bond et al., 2015; Kahru et al., 2018). PC1 was the only PC that was significantly correlated with typical indices of ecosystem productivity including surface Chl *a* (Spearman's $\rho = -0.82$, $p = 9 \times 10^{-8}$) and vertically integrated NPP ($\rho = -0.84$, $p = 6 \times 10^{-9}$).

PC2 explained 25% of the variance and had strongly negative coefficients for Si_{ex} and surface dFe and a strongly positive coefficient for ferrocline depth (with weaker negative coefficients for N* and positive coefficients for NO_3^-, PO_4^{3-}, and NH_4^+). PC2 likely reflected surface Fe limitation in the CCE, with positive scores indicating Fe-depleted conditions with low surface dFe, a deep ferrocline, and Si $(OH)_4$ drawn down by Fe-starved diatoms. Positive PC2 (Fe limitation) was typically found at intermediate distances from the coast; the cycles conducted nearest to the coast and farthest from the coast typically had negative scores.

PC3 explained 15% of the variance and had strongly positive coefficients for surface Si $(OH)_4$, PO_4^{3-}, and Si_{ex} and negative coefficients for N* (Figure 1c,d). Despite the positive coefficients for these surface macronutrients, PC3 also had slightly positive coefficients for nitracline depth, silicacline depth, and phosphocline depth. It had near-zero coefficients for surface NO_3^-, dFe, and ferrocline depth. PC3 largely splits the data set into high PO_4^{3-}:NO_3^- and $Si(OH)_4$:NO_3^- and low PO_4^{3-}:NO_3^- and $Si(OH)_4$:NO_3^- cycles and showed the greatest variability in water parcels with positive values for PC1 (i.e., low nutrient). Notably, the four cycles with distinctly low PC3 scores (<−2) were either close to shore (two P1408 cycles) or on the coastal edges of high plankton biomass open-ocean frontal regions (one cycle each from P1106 and P1208). These cycles all exhibited very low concentrations of $Si(OH)_4$ (<0.56 μmol L^{-1}; four of the five lowest values in the data set) and PO_4^{3-} (<0.22 μmol L^{-1}, the four lowest values in the data set). In contrast, cycles with positive PC1 and PC3 were typically far from shore in persistently oligotrophic regions.

The mechanisms responsible for generating the PC3 mode of variability are less obvious than for PC1 or PC2 but may reflect periods with preferential N recycling and hence export of Si- and P-enriched particles or periods following intense Si and P uptake by diatoms. Diatoms have been shown to have low N:P ratios in the Southern Ocean and in culture (Garcia et al., 2018; Lomas et al., 2019; Price, 2005; Quigg et al., 2003). Their non-Redfieldian growth could thus preferentially drawdown PO_4^-, relative to NO_3^-. Maintenance of low P:N conditions would then require that the P (and Si) enriched particulate matter be subsequently exported to depth, rather than remineralized within the euphotic zone, an outcome that is likely given the demonstrated importance of diatoms to the biological pump in the CCE (Brzezinski et al., 2015; Krause et al., 2015; Shipe et al., 2002). An alternative or potentially complementary mechanism involves preferential recycling of N relative to P and Si. Preferential recycling of N relative to P may be caused by the consistent pattern of excess PO_4^{3-} relative to NO_3^- in the CCE (e.g., negative N*), which suggests a generally N-limited community.

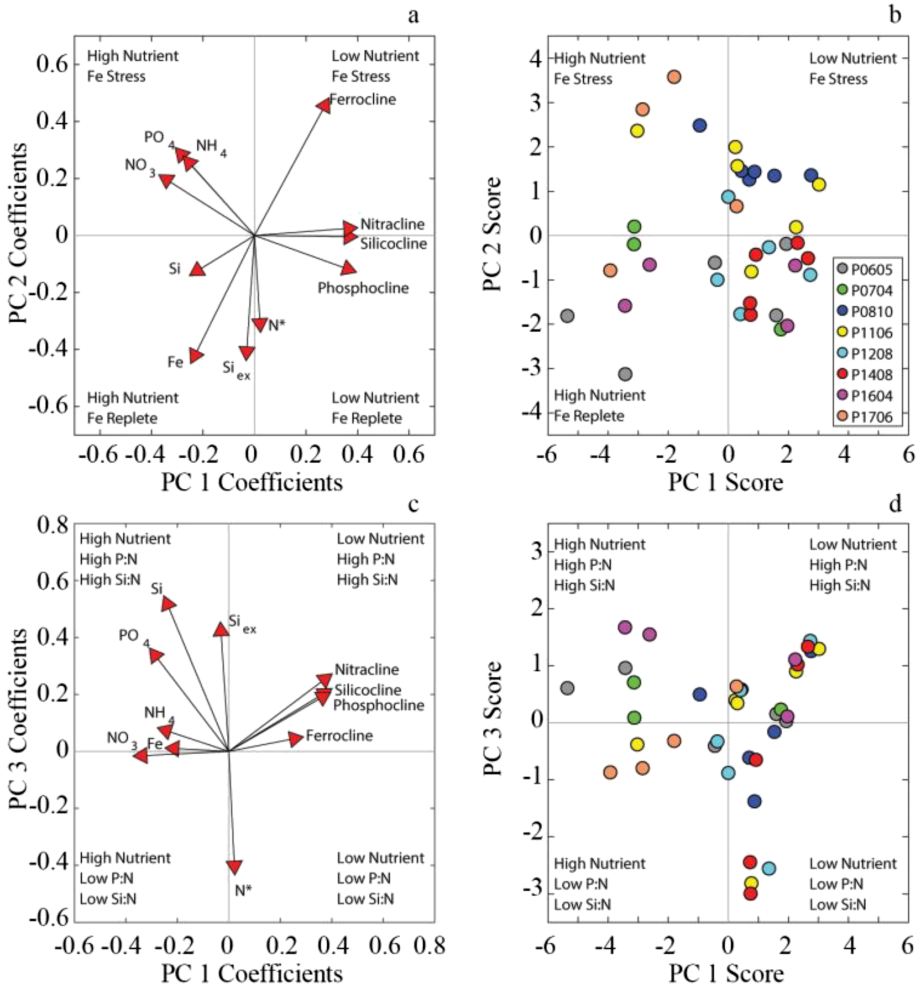

Figure 1. Probabilistic principal component analysis of nutrient landscape based on cycle average surface nutrients and depths of nutriclines. (a) Coefficients for principal component (PC) 1 and PC2 for all 11 variables. Upper left quadrant reflects high-nutrient, Fe stress conditions. Upper right quadrant is low-nutrient, Fe stress. Lower left is high-nutrient, Fe-replete. Lower right is low-nutrient, Fe-replete. (b) PC1 and PC2 scores for all 38 cycles. Color denotes cruise. (c) PC1 and PC3 coefficients. (d) PC1 and PC3 scores.

Preferential recycling of N relative to Si is expected because Si dissolution from sinking particles is primarily a (relatively slow) physicochemical process, while N recycling is mediated by microbes and zooplankton that preferentially consume amino acids relative to lipids and other recalcitrant forms of organic matter. Thus when sinking particles are removing organic matter from the surface ocean, preferential N recycling could lead to reduced PO_4^{3-}:NO_3^- and $Si(OH)_4$:NO_3^- ratios due to export of high P:N and Si:N particles. Conversely, periods of reduced N recycling or reduced export of diatoms would be associated with less downward flux of silicon- or phosphorus-enriched organic matter. In such cases, drawdown of the limiting nutrient (N) by phytoplankton would lead to high PO_4^{3-}:NO_3^- and $Si(OH)_4$:NO_3^- ratios in surface waters. These hypotheses are supported by the Si:N ratio of sinking particles, which was typically greater than 1, particularly in high biomass areas (when Chl >0.5 mg Chl a m^{-3}, the mean Si:N ratio was 3.4 (mol:mol) and the median was 3.2). PC3 may thus reflect a mechanism that may generate Si_{ex} without Fe limitation, although it notably explains less of the variability in the Si_{ex} signal than PC2 (Fe limitation). It is important to note, however, that we do not have measurements of P:N ratios of sinking material. N:P ratios of sinking material are variable in the world oceans, with some regions showing excess P export and other regions showing excess N export (Benitez-Nelson et al., 2004; Sekula-Wood et al., 2012; Singh et al., 2015; Stukel et al., 2016). Differences may depend on whether total N flux is

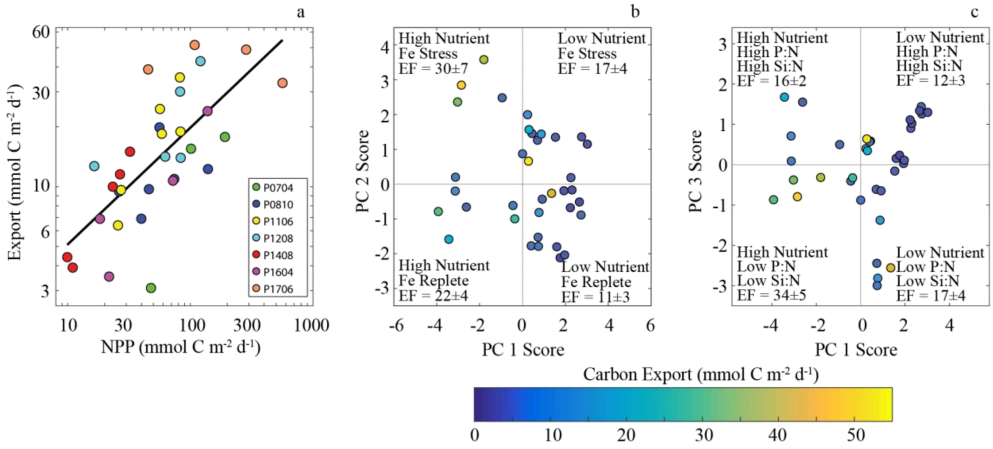

Figure 2. Vertical carbon flux as a function of NPP (a), PC1 and PC2 (b), and PC1 and PC3 (c). OLS regression line in (a) is $\log_{10}(\text{Export}) = 0.59 \times \log_{10}(\text{NPP}) + 0.12$. Color bar depicts export values in (b) and (c). EF denotes the export flux in each quadrant (mean ± standard error, units of mmol C m^{-2} d^{-1}).

compared to organic P flux (in which case excess P remineralization is typically found) or to total P flux (which at times shows excess P export) (Faul et al., 2005; Hopkinson & Vallino, 2005). The surprising pattern of positive coefficients for both surface Si $(OH)_4$ and depth of the silicocline and surface PO_4^{3-} and depth of the phosphocline also suggest, however, that altered stratification and/or subsurface nutrient supply could play a role in this mode of variability.

3.2. BCP Responses to the Nutrient Landscape and NPP

NPP is generally considered to be the best ecosystem predictor of vertical carbon export. Indeed, most models assume a relationship between NPP and export and then focus on estimating export efficiency (export/NPP) as a function of NPP, temperature, and/or the size-structure of phytoplankton communities (Henson et al., 2011; Laws et al., 2011; Siegel et al., 2014). An OLS regression of $\log_{10}$-transformed export against $\log_{10}$-transformed NPP suggested a relationship of $\text{Export} = 1.3 \times \text{NPP}^{0.59}$ (Figure 2a). The fact that the exponent in this equation is less than one implies that export efficiency (also called the e-ratio) decreases with increasing NPP. This inverse relationship between export efficiency and NPP is notably different from the results of some prominent global algorithms used to predict carbon export (Dunne et al., 2005; Laws et al., 2000; Siegel et al., 2014) but is not dissimilar to results quantifying intraregional variability in the BCP in other areas (Maiti et al., 2013). The regression in Figure 2a explains a moderate amount of the variability in export ($R^2 = 0.49$).

We compared mean carbon export under different nutrient conditions (Figure 2b, c). Carbon export was substantially higher during high-nutrient conditions, especially during Fe-stressed conditions (upper left quadrant of Figure 2b, export = 30 ± 7 mmol C m^{-2} d^{-1}, mean ± standard error) and low PO_4^{3-}:NO_3^- and $Si(OH)_4$:NO_3^- cycles (lower left quadrant of Figure 2c, export = 34 ± 4.6 mmol C m^{-2} d^{-1}). Carbon export was lower during high-nutrient but Fe-replete (22 ± 3.6 mmol C m^{-2} d^{-1}) or high PO_4^{3-}:NO_3^- and $Si(OH)_4$:NO_3^- cycles (16 ± 2.3 mmol C m^{-2} d^{-1}). During low-nutrient conditions (PC1 > 0, all quadrants had mean export ranging from 11 to 17 mmol C m^{-2} d^{-1}). These results agree with previous studies finding that export in the CCE is enhanced during Fe-limited conditions (Brzezinski et al., 2015; Stukel et al., 2017). They also support the supposition that PC3 is driven by preferential N recycling; when export is high, preferential N recycling can lead to low PO_4^{3-}:NO_3^- and Si $(OH)_4$:NO_3^-. When export is low, the Si- and P-enriched organic matter is not efficiently removed from the ecosystem, limiting the impact of preferential N recycling. These results are not, however, inconsistent with our alternate or complementary hypothesis for PC3 (excess P and Si drawdown during non-Redfieldian diatom blooms and subsequent export of P- and Si-enriched particles). Importantly, this suggests that PC1 (system eutrophy) and PC2 (Fe stress) may drive carbon export patterns, while PC3 may result from variability in particle export. Further research is necessary to support or refute these hypotheses.

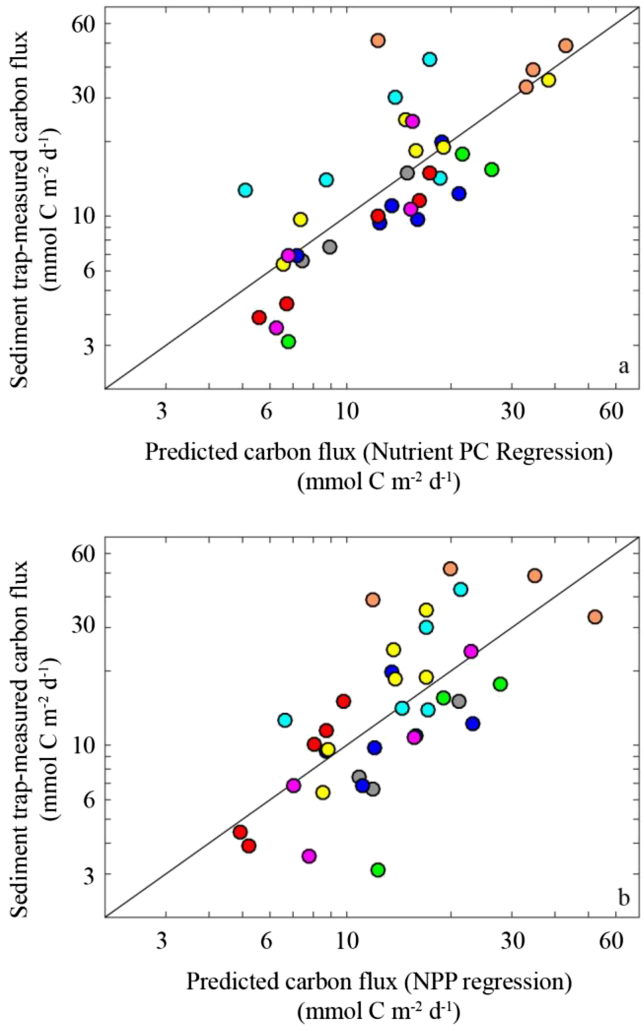

Figure 3. Comparison of sediment trap-measured carbon flux to carbon flux predicted using regressions based on nutrient principal components (a) or NPP (b). OLS regression in (a) is $\log_{10}(\text{Export}) = -0.089 \times \text{PC1} + 0.060 \times \text{PC2} + -0.093 \times \text{PC3} + 1.14$. OLS regression in (b) is $\log_{10}(\text{Export}) = 0.59 \times \text{NPP} + 0.11$.

To determine which PCs should be included as predictors of carbon export, we used step-wise linear regression. Results showed that PC1, PC2, and PC3 should all be included (with p values of 3.5×10^{-5}, 0.021, and 0.004, respectively) but that PC4 did not have statistically significant predictive value ($p = 0.90$). The resultant equation was $\log_{10}(\text{export}) = -0.089 \times \text{PC1} + 0.060 \times \text{PC2} + -0.093 \times \text{PC3} + 1.14$. The R^2 for this equation was 0.59, which suggests that the nutrient landscape may be a better predictor of export flux than NPP (Figure 3). However, the additional independent variables in the PC regression make a simple R^2 comparison problematic. To statistically compare the PC and NPP regressions, we used a nonparametric bootstrapping approach using withheld data points as an independent validation. We tested models with PC1, PC1 and PC2 or PC3, the first three PCs, and NPP. All PC models outperformed the NPP model with respect to the sum of squared misfits, except the model including all three PCs (which was a better predictor in only 37% of simulations). The model with PC1 only was better than the NPP model in 73% of simulations. The model with PC1 and PC2 was better in 63% of simulations. The model with PC1 and PC3 was better in 90% of simulations. Our results thus suggest that measurements of the nutrient landscape may prove to be a useful predictor of carbon export.

3.3. Fe Stress and Carbon Export Efficiency

Our results confirm that negative values of Si_{ex} in the CCE are primarily correlated with Fe-limited conditions (PC2), although they can be created to a lesser extent by preferential remineralization of N (PC3). They also agree with previous results suggesting that physiological adaptations of Fe-stressed diatoms may lead to increased silicification and efficient export of this Si-ballasted material (Bruland et al., 2001; Brzezinski et al., 2015). These results may shed light on surprising patterns that have emerged with respect to the relationship between primary productivity and export efficiency (export/primary productivity). Early syntheses and models suggested that export efficiency should be higher in productive regions (Dunne et al., 2005; Eppley & Peterson, 1979; Laws et al., 2000). These results were informed by measurements of new production, which show a strong correlation between nitrate, productivity, and export efficiency (Dugdale & Goering, 1967; Harrison et al., 1987), and by the consensus view that large phytoplankton in upwelling regions are more likely to sink individually or be consumed by large fecal pellet-producing mesozooplankton (Michaels & Silver, 1988; Smayda, 1970). More recent results, however, have found inverse correlations between primary productivity and export efficiency in the CCE (Kelly et al., 2018; Stukel et al., 2013) and other regions including the Southern Ocean, Canary Current, and Gulf of Mexico (Hernández-León et al., 2019; Maiti et al., 2013; Maiti et al., 2016). Hypothesized reasons for this discrepancy between theory and in situ measurements include offshore advection of communities, temporal lags between production and export, and specific relationships associated with zooplankton and microbes (Henson et al., 2015; Kelly et al., 2018; Laws & Maiti, 2019; Le Moigne et al., 2016; Plattner et al., 2005). Temporal lags between phytoplankton production and the conversion of organic matter into sinking particles by multiple food web pathways, which range from two to thirty days, may be of particular importance and have been shown to explain inverse relationships in the Southern Ocean and oligotrophic Pacific (Benitez-Nelson et al., 2001; Laws & Maiti, 2019; Stange et al., 2017). However, comparison of satellite-derived NPP time series to in situ export measurements in the CCE suggested that although there was on average a 7- to 8-day lag between production and export, this lag could not explain the inverse relationship in our carbon flux data set (Kahru et al., 2019). Instead, our results suggest changes in physiological status over the course of a bloom may also contribute substantially, at least in potentially Fe-limited regions. Primary production (and new production) peak during the early phases of a bloom when nutrients are

replete. During these periods healthy cells are able to regulate their buoyancy either actively or passively. In the mid to late stages of the bloom, however, decreased primary production coincides with Fe stress-induced increases in density and sinking rates. This decouples export from contemporaneous primary productivity, obfuscating expected relationships between productivity and export.

4. Conclusions

PCA showed that the dominant mode of nutrient variability in the CCE was an upwelling-driven onshore-offshore nutrient gradient. The second mode of variability reflected Fe stress as evidenced by a strong covariance between Si_{ex} and surface dFe concentrations. This supports the use of negative Si_{ex} as a tracer of Fe stress in the region. However, the third PC was associated with Si_{ex} (and N*), but not dFe. We interpret this as a signal of negative Si_{ex} creation through either non-Redfieldian nutrient uptake by diatoms or preferential recycling of N relative to Si in the surface ocean. Vertical carbon export was enhanced during high-nutrient, Fe-stressed, and low PO_4^{3-}:NO_3^- conditions. Linear regressions relating vertical carbon flux to nutrient PCs explained more of the variance and had higher predictive power than a linear regression between NPP and export. This suggests that nutrient concentrations could be used to predict carbon export, although we caution that such relationships are likely region-specific and future work is necessary to determine if they are robust across seasonal and interannual variability in the CCE.

Acknowledgments
We thank the captains and crews of the R/Vs Knorr, Thompson, Melville, Revelle, and Sikuliaq. We are also indebted to our many colleagues in the CCE LTER Program, especially Ralf Goericke, Shonna Dovel, and Megan Roadman who were responsible for NPP and macronutrient measurements. All data used in this manuscript are available on the CCE LTER DataZoo website: https://oceaninformatics.ucsd.edu/datazoo/catalogs/ccelter/datasets. This research was supported by National Science Foundation grants OCE-0417616, OCE-1026607, OCE-1637632, and OCE-1614359. A portion of this work was performed at the National High Magnetic Field Laboratory, which is supported by National Science Foundation Cooperative Agreement No. DMR-1644779 and the State of Florida.

References

Bakun, A. (1990). Global climate change and intensification of coastal ocean upwelling. *Science*, *247*(4939), 198–201. https://doi.org/10.1126/science.247.4939.198

Behrenfeld, M. J., Bale, A. J., Kolber, Z. S., Aiken, J., & Falkowski, P. G. (1996). Confirmation of iron limitation of phytoplankton photosynthesis in the equatorial Pacific Ocean. *Nature*, *383*(6600), 508–511.

Benitez-Nelson, C. R. (2000). The biogeochemical cycling of phosphorus in marine systems. *Earth Science Reviews*, *51*(1-4), 109–135.

Benitez-Nelson, C. R., Buesseler, K. O., Karl, D. M., & Andrews, J. (2001). A time-series study of particulate matter export in the North Pacific Subtropical Gyre based on Th-234: U-238 disequilibrium. *Deep-Sea Research Part I*, *48*(12), 2595–2611.

Benitez-Nelson, C. R., O'Neill, L., Kolowith, L. C., Pellechia, P., & Thunell, R. (2004). Phosphonates and particulate organic phosphorus cycling in an anoxic marine basin. *Limnology and Oceanography*, *49*(5), 1593–1604.

Bograd, S. J., Buil, M. P., Di Lorenzo, E., Castro, C. G., Schroeder, I. D., Goericke, R., et al. (2015). Changes in source waters to the Southern California Bight. *Deep-Sea Res. II*, *112*, 42–52.

Bond, N. A., Cronin, M. F., Freeland, H., & Mantua, N. (2015). Causes and impacts of the 2014 warm anomaly in the NE Pacific. *Geophysical Research Letters*, *42*, 3414–3420. https://doi.org/10.1002/2015GL063306

Boyd, P. W. (2015). Toward quantifying the response of the oceans' biological pump to climate change. *Frontiers in Marine Science*, *2*, 77.

Boyd, P. W., Claustre, H., Levy, M., Siegel, D. A., & Weber, T. (2019). Multi-faceted particle pumps drive carbon sequestration in the ocean. *Nature*, *568*(7752), 327–335. https://doi.org/10.1038/s41586-019-1098-2

Bruland, K. W., Rue, E. L., & Smith, G. J. (2001). Iron and macronutrients in California coastal upwelling regimes: Implications for diatom blooms. *Limnology and Oceanography*, *46*(7), 1661–1674.

Brzezinski, M. A., Krause, J. W., Bundy, R. M., Barbeau, K. A., Franks, P., Goericke, R., et al. (2015). Enhanced silica ballasting from iron stress sustains carbon export in a frontal zone within the California Current. *Journal of Geophysical Research, Oceans*: *120*, 4654–4669. https://doi.org/10.1002/2015JC010829

Buesseler, K. O., & Boyd, P. W. (2009). Shedding light on processes that control particle export and flux attenuation in the twilight zone of the open ocean. *Limnology and Oceanography*, *54*(4), 1210–1232.

Bundy, R. M., Jiang, M., Carter, M., & Barbeau, K. A. (2016). Iron-binding ligands in the southern California current system: Mechanistic studies. *Frontiers in Marine Science*, *3*, 27.

Chelton, D. B., Bernal, P., & McGowan, J. A. (1982). Large-scale interannual physical and biological interaction in the California Current. *Journal of Marine Research*, *40*(4), 1095–1125.

Davey, M., Tarran, G. A., Mills, M. M., Ridame, C., Geider, R. J., & LaRoche, J. (2008). Nutrient limitation of picophytoplankton photosynthesis and growth in the tropical North Atlantic. *Limnology and Oceanography*, *53*(5), 1722–1733.

de Baar, H. J. W., Boyd, P.W., Coale, K.H., Boyd, P.W., Tsuda, A., Boyd, P.W., Assmy, P., et al. (2005). Synthesis of iron fertilization experiments: From the iron age in the age of enlightenment. *Journal of Geophysical Research:Oceans*, *110*, C09S16. https://doi.org/10.1029/2004JC002601

de Verneil, A., & Franks, P. J. S. (2015). A pseudo-Lagrangian method for remapping ocean biogeochemical tracer data: Calculation of net Chl-a growth rates. *Journal of Geophysical Research:Oceans*, *120*, 4962–4979. https://doi.org/10.1002/2015JC010898

Draper, N. R., & Smith, H. (1998). *Applied regression analysis*. Hoboken, NJ: John Wiley & Sons.

Ducklow, H. W., & McCallister, S. L. (2004). The biogeochemistry of carbon dioxide in the coastal oceans. In A. R. Robinson, K. Brink, & B. J. Rothschild (Eds.), *The global coastal ocean: Multiscale interdisciplinary processes* (pp. 269–315). Cambridge, MA: Harvard University Press.

Ducklow, H. W., Steinberg, D. K., & Buesseler, K. O. (2001). Upper ocean carbon export and the biological pump. *Oceanography*, *14*(4), 50–58.

Dugdale, R. C. (1967). Nutrient limitation in the sea: Dynamics, identification, and significance. *Limnology and Oceanography*, *12*(4), 685–695.

Dugdale, R. C., & Goering, J. J. (1967). Uptake of new and regenerated forms of nitrogen in primary productivity. *Limnology and Oceanography*, *12*(2), 196–206.

Dunne, J. P., Armstrong, R. A., Gnanadesikan, A., & Sarmiento, J. L. (2005). Empirical and mechanistic models for the particle export ratio. *Global Biogeochemical Cycles*, *19*(4), GB4026. https://doi.org/10.1029/2004GB002390

Eppley, R. W., & Peterson, B. J. (1979). Particulate organic matter flux and planktonic new production in the deep ocean. *Nature*, *282*(5740), 677–680.

Falkowski, P. G., Barber, R. T., & Smetacek, V. (1998). Biogeochemical controls and feedbacks on ocean primary production. *Science*, *281*(5374), 200–207. https://doi.org/10.1126/science.281.5374.200

Faul, K. L., Paytan, A., & Delaney, M. L. (2005). Phosphorus distribution in sinking oceanic particulate matter. *Marine Chemistry*, *97*(3-4), 307–333.

Franck, V. M., Brzezinski, M. A., Coale, K. H., & Nelson, D. M. (2000). Iron and silicic acid concentrations regulate Si uptake north and south of the Polar Frontal Zone in the Pacific Sector of the Southern Ocean. *Deep Sea Research Part II: Topical Studies in Oceanography*, *47*(15-16), 3315–3338.

Garcia, N. S., Sexton, J., Riggins, T., Brown, J., Lomas, M. W., & Martiny, A. C. (2018). High variability in cellular stoichiometry of carbon, nitrogen, and phosphorus within classes of marine eukaryotic phytoplankton under sufficient nutrient conditions. *Frontiers in Microbiology*, *9*, 543.

Harrison, W. G., Platt, T., & Lewis, M. R. (1987). *f*-ratio and its relationship to ambient nitrate concentration in coastal waters. *Journal of Plankton Research*, *9*(1), 235–248.

Henson, S. A., Sanders, R., Madsen, E., Morris, P. J., Le Moigne, F., & Quartly, G. D. (2011). A reduced estimate of the strength of the ocean's biological carbon pump. *Geophysical Research Letters*, *38*, L04606. https://doi.org/10.1029/2011GL046735

Henson, S. A., Yool, A., & Sanders, R. (2015). Variability in efficiency of particulate organic carbon export: A model study. *Global Biogeochemical Cycles*, *29*, 33–45. https://doi.org/10.1002/2014GB004965

Hernández-León, S., Putzeys, S., Almeida, C., Bécognée, P., Marrero-Díaz, A., Arístegui, J., & Yebra, L. (2019). Carbon export through zooplankton active flux in the Canary Current. *Journal of Marine Systems*, *189*, 12–21.

Hogle, S. L., Dupont, C.L., Boyd, P.W., Hopkinson, B.M., Boyd, P.W., King, A.L., Boyd, P.W., Buck, K.N., Boyd, P.W., Roe, K.L., et al. (2018). Pervasive iron limitation at subsurface chlorophyll maxima of the California Current. *Proceedings of the National Academy of Sciences*, *115*(52), 13,300–13,305.

Hopkinson, C. S. Jr., & Vallino, J. J. (2005). Efficient export of carbon to the deep ocean through dissolved organic matter. *Nature*, *433*(7022), 142–145. https://doi.org/10.1038/nature03191

Hutchins, D. A., & Bruland, K. W. (1998). Iron-limited diatom growth and Si: N uptake ratios in a coastal upwelling regime. *Nature*, *393*(6685), 561–564.

Johnson, K. S., Elrod, V., Fitzwater, S., Plant, J., Boyle, E., Bergquist, B., et al. (2007). Developing standards for dissolved iron in seawater, *Eos. Transactions of the American Geophysical Union*, *88*(11), 131–132.

Kahru, M., Goericke, R., Kelly, T. B., & Stukel, M. R. (2019). Satellite estimation of carbon export by sinking particles in the California Current calibrated with sediment trap data. *Deep Sea Research, Part II*. https://doi.org/10.1016/j.dsr1012.2019.104639

Kahru, M., Jacox, M. G., & Ohman, M. D. (2018). CCE1: Decrease in the frequency of oceanic fronts and surface chlorophyll concentration in the California Current System during the 2014–2016 northeast Pacific warm anomalies. *Deep-Sea Research Part I*, *140*, 4–13. https://doi.org/10.1016/j.dsr.2018.04.007

Kelly, T. B., Goericke, R., Kahru, M., Song, H., & Stukel, M. R. (2018). CCE II: Spatial and interannual variability in export efficiency and the biological pump in an eastern boundary current upwelling system with substantial lateral advection. *Deep-Sea Research Part I*, *140*, 14–25.

King, A. L., & Barbeau, K. (2007). Evidence for phytoplankton iron limitation in the southern California Current System. *Marine Ecology Progress Series*, *342*, 91–103.

King, A. L., & Barbeau, K. A. (2011). Dissolved iron and macronutrient distributions in the southern California Current System. *Journal of Geophysical Research:Oceans*, *116*, C03018. https://doi.org/10.1029/2010JC006324

King, A. L., Buck, K. N., & Barbeau, K. A. (2012). Quasi-Lagrangian drifter studies of iron speciation and cycling off Point Conception, California. *Marine Chemistry*, *128–129*, 1–12.

Knauer, G. A., Martin, J. H., & Bruland, K. W. (1979). Fluxes of particulate carbon, nitrogen, and phosphorus in the upper water column of the Northeast Pacific. *Deep-Sea Research*, *26*(1), 97–108.

Krause, J. W., Brzezinski, M. A., Goericke, R., Landry, M. R., Ohman, M. D., Stukel, M. R., & Taylor, A. G. (2015). Variability in diatom contributions to biomass, organic matter production and export across a frontal gradient in the California Current Ecosystem. *Journal of Geophysical Research:Oceans*, *120*, 1032–1047. https://doi.org/10.1002/2014JC010472

Landry, M. R., Ohman, M. D., Goericke, R., Stukel, M. R., Barbeau, K. A., Bundy, R., & Kahru, M. (2012). Pelagic community responses to a deep-water front in the California Current Ecosystem: Overview of the A-Front Study. *Journal of Plankton Research*, *34*(9), 739–748.

Landry, M. R., Ohman, M. D., Goericke, R., Stukel, M. R., & Tsyrklevich, K. (2009). Lagrangian studies of phytoplankton growth and grazing relationships in a coastal upwelling ecosystem off Southern California. *Progress in Oceanography*, *83*, 208–216.

Lavaniegos, B. E., & Ohman, M. D. (2007). Coherence of long-term variations of zooplankton in two sectors of the California Current System. *Progress in Oceanography*, *75*(1), 42–69.

Laws, E. A., D'Sa, E., & Naik, P. (2011). Simple equations to estimate ratios of new or export production to total production from satellite-derived estimates of sea surface temperature and primary production. *Limnology and Oceanography: Methods*, *9*(12), 593–601. https://doi.org/10.4319/lom.2011.9.593

Laws, E. A., Falkowski, P. G., Smith, W. O., Ducklow, H., & McCarthy, J. J. (2000). Temperature effects on export production in the open ocean. *Global Biogeochemical Cycles*, *14*(4), 1231–1246.

Laws, E. A., & Maiti, K. (2019). The relationship between primary production and export production in the ocean: Effects of time lags and temporal variability. *Deep-Sea Research Part I*, *148*, 100–107. https://doi.org/10.1016/j.dsr.2019.05.006

Le Moigne, F. A., Henson, S. A., Cavan, E., Georges, C., Pabortsava, K., Achterberg, E. P., et al. (2016). What causes the inverse relationship between primary production and export efficiency in the Southern Ocean? *Geophysical Research Letters*, *43*, 4457–4466. https://doi.org/10.1002/2016GL068480

Lomas, M. W., Baer, S., Acton, S., & Krause, J. W. (2019). Pumped up by the cold: Elemental quotas and stoichiometry of cold-water diatoms. *Frontiers in Marine Science*, *6*, 197.

Maiti, K., Bosu, S., D'Sa, E. J., Adhikari, P. L., Sutor, M., & Longnecker, K. (2016). Export fluxes in northern Gulf of Mexico—Comparative evaluation of direct, indirect and satellite-based estimates. *Marine Chemistry*, *184*, 60–77.

Maiti, K., Charette, M. A., Buesseler, K. O., & Kahru, M. (2013). An inverse relationship between production and export efficiency in the Southern Ocean. *Geophysical Research Letters*, *40*, 1557–1561. https://doi.org/10.1002/GRL.50219

McGowan, J. A., Bograd, S. J., Lynn, R. J., & Miller, A. J. (2003). The biological response to the 1977 regime shift in the California Current. *Deep-Sea Research Part II*, *50*(14-16), 2567–2582.
Michaels, A. F., & Silver, M. W. (1988). Primary production, sinking fluxes and the microbial food web. *Deep-Sea Research*, *35*(4), 473–490.
Moore, C. M., Mills, M. M., Arrigo, K. R., Berman-Frank, I., Bopp, L., Boyd, P. W., et al. (2013). Processes and patterns of oceanic nutrient limitation. *Nature Geoscience*, *6*(9), 701–710. https://doi.org/10.1038/ngeo1765
Morrow, R. M., Ohman, M. D., Goericke, R., Kelly, T. B., Stephens, B. M., & Stukel, M. R. (2018). Primary productivity, mesozooplankton grazing, and the biological pump in the California Current Ecosystem: Variability and Response to El Niño. *Deep-Sea Research Part I*, *140*, 52–62.
Nickels, C. F., & Ohman, M. D. (2018). CCEIII: Persistent functional relationships between copepod egg production rates and food concentration through anomalously warm conditions in the California Current Ecosystem. *Deep-Sea Research Part I*, *140*, 26–35. https://doi.org/10.1016/j.dsr.2018.07.001
Ohman, M. D., Barbeau, K., Franks, P. J. S., Goericke, R., Landry, M. R., & Miller, A. J. (2013). Ecological transitions in a coastal upwelling ecosystem. *Oceanography*, *26*(3), 210–219. https://doi.org/10.5670/oceanog.2013.65
Omta, A. W., Bruggeman, J., Kooijman, S. A. L. M., & Dijkstra, H. A. (2006). Biological carbon pump revisited: Feedback mechanisms between climate and the Redfield ratio. *Geophysical Research Letters*, *33*, L14613. https://doi.org/10.1029/2006GL026213
Owens, S. A., Buesseler, K. O., & Sims, K. W. W. (2011). Re-evaluating the ^{238}U-salinity relationship in seawater: Implications for the ^{238}U-^{234}Th disequilibrium method. *Marine Chemistry*, *127*(1-4), 31–39.
Pabortsava, K., Lampitt, R. S., Benson, J., Crowe, C., McLachlan, R., Le Moigne, F. A., et al. (2017). Carbon sequestration in the deep Atlantic enhanced by Saharan dust. *Nature Geoscience*, *10*(3), 189.
Parsons, T., Maita, Y., & Lalli, C. (1984). *A manual of chemical and biological methods for seawater analysis* (p. 172). Oxford, UK: Pergamon Press.
Passow, U., & Carlson, C. A. (2012). The biological pump in a high CO_2 world. *Marine Ecology Progress Series*, *470*, 249–271.
Pike, S. M., Buesseler, K. O., Andrews, J., & Savoye, N. (2005). Quantification of ^{234}Th recovery in small volume sea water samples by inductively coupled plasma-mass spectrometry. *Journal of Radioanalytical and Nuclear Chemistry*, *263*(2), 355–360.
Plattner, G. K., Gruber, N., Frenzel, H., & McWilliams, J. C. (2005). Decoupling marine export production from new production. *Geophysical Research Letters*, *32*, L11612. https://doi.org/10.1029/2005GL022660
Price, N. M. (2005). The elemental stoichiometry and composition of an iron-limited diatom. *Limnology and Oceanography*, *50*(4), 1159–1171.
Quigg, A., Finkel, Z. V., Irwin, A. J., Rosenthal, Y., Ho, T.-Y., Reinfelder, J. R., et al. (2003). The evolutionary inheritance of elemental stoichiometry in marine phytoplankton. *Nature*, *425*(6955), 291–294. https://doi.org/10.1038/nature01953
Redfield, A. C. (1934). On the proportions of organic derivatives in sea water and their relation to the composition of plankton. In R. J. Daniel (Ed.), *James Johnson Memorial Volume* (pp. 177–192). U. K.: Liverpool.
Rykaczewski, R. R., & Dunne, J. P. (2010). Enhanced nutrient supply to the California Current Ecosystem with global warming and increased stratification in an earth system model. *Geophysical Research Letters*, *37*, L21606. https://doi.org/10.1029/2010GL045019
Savoye, N., Benitez-Nelson, C., Burd, A. B., Cochran, J. K., Charette, M., Buesseler, K. O., et al. (2006). ^{234}Th sorption and export models in the water column: A review. *Marine Chemistry*, *100*(3-4), 234–249.
Sekula-Wood, E., Benitez-Nelson, C. R., Bennett, M. A., & Thunell, R. (2012). Magnitude and composition of sinking particulate phosphorus fluxes in Santa Barbara Basin, California. *Global Biogeochemical Cycles*, *26*, GB2023. https://doi.org/10.1029/2011GB004180
Shipe, R. F., Passow, U., Brzezinski, M. A., Graham, W. M., Pak, D. K., Siegel, D. A., & Alldredge, A. L. (2002). Effects of the 1997-98 El Niño on seasonal variations in suspended and sinking particles in the Santa Barbara basin. *Progress in Oceanography*, *54*(1-4), 105–127.
Siegel, D. A., Buesseler, K. O., Doney, S. C., Sailley, S. F., Behrenfeld, M. J., & Boyd, P. W. (2014). Global assessment of ocean carbon export by combining satellite obervations and food-web models. *Global Biogeochemical Cycles*, *28*, 181–196. https://doi.org/10.1002/2013GB004743
Singh, A., Baer, S., Riebesell, U., Martiny, A., & Lomas, M. (2015). C: N: P stoichiometry at the Bermuda Atlantic Time-series Study station in the North Atlantic Ocean. *Biogeosciences*, *12*(21), 6389–6403.
Smayda, T. J. (1970). The suspension and sinking of phytoplankton in the sea. *Oceanography and Marine Biology. Annual Review*, *8*, 353–414.
Sokal, R. R., & Rohlf, F. J. (2012). Biometry: The principles and practice of statistics in biological research (4th ed.). *,W.H.* New York: Freeman and Company.
Stange, P., Bach, L. T., Le Moigne, F. A., Taucher, J., Boxhammer, T., & Riebesell, U. (2017). Quantifying the time lag between organic matter production and export in the surface ocean: Implications for estimates of export efficiency. *Geophysical Research Letters*, *44*, 268–276. https://doi.org/10.1002/2016GL070875
Steinberg, D. K., & Landry, M. R. (2017). Zooplankton and the ocean carbon cycle. *Annual Review of Marine Science*, *9*, 413–444. https://doi.org/10.1146/annurev-marine-010814-015924
Stukel, M. R., Aluwihare, L. I., Barbeau, K. A., Chekalyuk, A. M., Goericke, R., Miller, A. J., et al. (2017). Mesoscale ocean fronts enhance carbon export due to gravitational sinking and subduction. *Proceedings of the National Academy of Sciences*, *114*(6), 1252–1257. https://doi.org/10.1073/pnas.1609435114
Stukel, M. R., Benitez-Nelson, C., Décima, M., Taylor, A. G., Buchwald, C., & Landry, M. R. (2016). The biological pump in the Costa Rica Dome: An open ocean upwelling system with high new production and low export. *Journal of Plankton Research*, *38*(2), 348–365. https://doi.org/10.1093/plankt/fbv097
Stukel, M. R., & Kelly, T. B. (2019). The Carbon:^{234}Thorium ratios of sinking particles in the California Current Ecosystem 2: Examination of a thorium sorption, desorption, and particle transport model. *Marine Chemistry*, *211*, 37–51.
Stukel, M. R., Kelly, T. B., Aluwihare, L. I., Barbeau, K. A., Goericke, R., Krause, J. W., et al. (2019). The Carbon:^{234}Thorium ratios of sinking particles in the California Current Ecosystem 1: Relationships with plankton ecosystem dynamics. *Marine Chemistry*, *212*, 1–15.
Stukel, M. R., Landry, M. R., Ohman, M. D., Goericke, R., Samo, T., & Benitez-Nelson, C. R. (2012). Do inverse ecosystem models accurately reconstruct plankton trophic flows? Comparing two solution methods using field data from the California Current. *Journal of Marine Systems*, *91*(1), 20–33.
Stukel, M. R., Ohman, M. D., Benitez-Nelson, C. R., & Landry, M. R. (2013). Contributions of mesozooplankton to vertical carbon export in a coastal upwelling system. *Marine Ecology Progress Series*, *491*, 47–65.
Sydeman, W. J., García-Reyes, M., Schoeman, D. S., Rykaczewski, R. R., Thompson, S. A., Black, B. A., & Bograd, S. J. (2014). Climate change and wind intensification in coastal upwelling ecosystems. *Science*, *345*(6192), 77–80. https://doi.org/10.1126/science.1251635

Takahashi, T., Broecker, W. S., & Langer, S. (1985). Redfield ratio based on chemical data from isopycnal surfaces. *Journal of Geophysical Research, Oceans*, *90*(NC4), 6907–6924.

Tipping, M. E., & Bishop, C. M. (1999). Probabilistic principal component analysis. *Journal of the Royal Statistical Society, Series B (Statistical Methodology)*, *61*(3), 611–622.

Volk, T., & Hoffert, M. I. (1985). Ocean carbon pumps: Analysis of relative strengths and efficiencies in ocean-driven atmospheric CO2 changes. In E. T. Sundquist & W. S. Broeker (Eds.), *The carbon cycle and atmospheric CO2: Natural variations Archean to present* (pp. 99–110). Washington, DC: American Geophysical Union.

Waples, J. T., Benitez-Nelson, C., Savoye, N., Van der Loeff, M. R., Baskaran, M., & Gustafsson, O. (2006). An introduction to the application and future use of ^{234}Th in aquatic systems. *Marine Chemistry*, *100*(3-4), 166–189.